Time dependence of the polarization of short X-ray pulses after crystal reflection

Walter Graeff

Hamburger Synchrotronstrahlungslabor Hasylab at Deutsches Elektronen-Synchrotron DESY, Hamburg, Germany.
E-mail: walter.graeff@desy.de

The short X-ray pulses coming out of a SASE FEL (self-amplified stimulated emission free-electron laser) have stimulated a closer inspection of the response of a crystal reflection to them. As the reflectivity of a crystal reflection depends on the polarization of the incident radiation, the time response does so as well. The response to a δ-pulse incident either under 45° linearly polarized with respect to the reflection plane of a monochromator crystal or circularly polarized is investigated in more detail. In contrast to the purely linear polarization perpendicular and parallel to the reflection plane, these mixed states show a very pronounced time dependence. In addition, a simulated SASE FEL bunch is investigated as an incident intensity distribution.

1. Introduction

The X-ray beam emerging from a free-electron laser (FEL) has a rather special time structure and can be either linearly polarized parallel to the magnetic field of the generating undulator or elliptically polarized if a helical undulator is used as a source. The numbers given here are valid for the XFEL, which is part of the linear collider project TESLA currently being proposed by DESY (1997). A similar project pursuing these synchrotron radiation sources in the X-ray regime, sometimes called fourth-generation sources, is planned in Stanford (SLAC, 1998).

Every 200 ms, a bunch train is released over 1 ms that consists of 11 315 bunches of length 180 fs. These bunches are subdivided in turn into bursts of coherent radiation with an average length of 0.1 fs.

The time response of a crystal to an incoming δ-pulse was calculated by Fourier transform of the plane-wave solutions given by dynamical theory, thereby following the approach of Shastri *et al.* (2001*a,b*). It transpired to be of the order of 10 fs for low-indexed reflections, significantly longer than the incident pulses.

As is well known from dynamical theory, when reflected, the incident radiation is subdivided into a component perpendicular (σ) and parallel (π) to the diffraction plane. Each component is reflected by the crystal with different strength, the difference expressed by the polarization factor $\cos(2\Theta_B)$, where Θ_B denotes the Bragg angle. The response time of the so-called π component is longer by this factor, and consequently the polarization of incident radiation that is not exactly polarized perpendicular or parallel to the plane of incidence must be strongly influenced.

It is the aim of this paper to investigate the time dependence of linearly polarized and elliptically polarized radiation, both for exemplary cases to demonstrate the effect. A detailed analysis of a given case is then straightforward.

2. Description of calculation

We follow the approach given by Shastri *et al.* (2001*a,b*). We begin by briefly recalling the formulae.

An arbitrary scalar wave may be considered as an appropriate superposition of plane waves:

$$E_{\text{in}}(\mathbf{r}, t) = \int \mathrm{d}^3 k \int \mathrm{d}\omega \tilde{E}(\mathbf{k}, \omega) \exp(i\,\mathbf{k}\mathbf{r} - i\omega t). \quad (1)$$

This very general expression is simplified in the following. The extremely long beamlines of an XFEL (several hundred metres) justify the assumption of a plane wave. If we are not too close to the border of the beam, we may also assume that the amplitude of the incident radiation is laterally independent of the position; in other words, the incident wave is laterally unlimited. Finally, we describe the short pulse as a δ-pulse and obtain

$$E_{\text{in}}(\mathbf{r}, t) = E_0\delta\left(t - \frac{\mathbf{K}_0^0}{|\mathbf{K}_0^0|}\frac{\mathbf{r}}{c}\right) = \frac{E_0}{2\pi}\int \mathrm{d}\omega \exp\left[i\omega\left(\frac{\mathbf{K}_0^0}{|\mathbf{K}_0^0|}\frac{\mathbf{r}}{c} - t\right)\right], \quad (2)$$

where $\mathbf{K}_0^0$ is chosen in such a way that it exactly fulfils the Bragg condition. The integral is running now over all frequencies. However, in practice, $\mathbf{K}_0^0$ belongs to a wave with a frequency of the order of $3 \times 10^{18}\,\text{s}^{-1}$ ($\omega_B/2\pi$), and a 0.03 fs-long pulse (three times shorter than the SASE pulses) corresponds to a frequency band of the order of $2.9 \times 10^{16}\,\text{s}^{-1}$, which is a deviation of roughly 1% (FWHM) around the central frequency. This frequency band is several orders of magnitude higher than the frequency band reflected by a crystal for a given direction of incidence. Although, formally, a δ-pulse involves all frequencies, limiting the integral to such a frequency band avoids some complications in using the results of dynamical theory. For a deviation that is too far from the central frequency, the curvature of the asymptotes should be taken into account, as should the fact that one of the assumptions of the two-wave case, namely that just two waves are predominant in the crystal, is no longer valid.

To find the response of a crystal reflection, we have to multiply in ν space each plane wave by its reflectivity factor $R(\omega)$, as given by dynamical theory, and transform the result back to the real space,

$$E_{\text{out}}(\mathbf{r}, t) = \frac{E_0}{2\pi}\int \mathrm{d}\omega R(\omega) \exp\left[i\omega\left(\frac{\mathbf{K}_h^0}{|\mathbf{K}_h^0|}\frac{\mathbf{r}}{c} - t\right)\right]. \quad (3)$$

We restrict ourselves further to the symmetric Bragg case. $R(\omega)$ is usually complex for a Bragg-case reflection.

We may neglect the trivial spatial dependence of the output signal by considering the signal at a fixed point, and we distinguish the two intrinsic polarization states by the subscripts σ and π, respectively. For the description of the polarization state we use the Stokes parameters and recall their definition,

$$\begin{aligned}
s_0 &= |E_\sigma|^2 + |E_\pi|^2, \\
s_1 &= |E_\sigma|^2 - |E_\pi|^2, \\
s_2 &= 2|E_\sigma||E_\pi|\cos\alpha, \\
s_3 &= 2|E_\sigma||E_\pi|\sin\alpha,
\end{aligned} \quad (4)$$

where α is the phase difference between the orthogonal components E_σ and E_π, and s_0 is the total intensity. The Stokes parameters $s_i, i = 1\ldots3$, describe the polarization state. $s_3 = 0$ indicates linear polarization, $s_3 > 0$ indicates right-handed elliptical polarization and $s_3 < 0$ indicates left-handed elliptical polarization.

The Stokes parameters are well suited for the characterization of the polarization state of a wave, the intensity of which is not varying with time. Unfortunately, when the total intensity has a time dependence, the Stokes parameters vary in time as well, thereby obscuring, eventually, the time dependence of the polarization state.

Therefore, normalizing the Stokes parameters by the intensity s_0 suppresses the intensity dependence completely and shows the polarization state more clearly. However, normalizing to too low an intensity overemphasizes features that are of less interest as they are not observable at all. Therefore, the normalized Stokes parameters s_{in} are set to zero where the intensity has dropped below 1% of its maximum. With $s_3 = 0$, $s_{1n} = 1$ means complete linear polarization in the σ direction, whereas $s_{1n} = -1$ means complete linear polarization in the π direction, and so on. For a detailed discussion, see Born & Wolf (1997). Note that the following is always true,

$$s_0^2 = s_1^2 + s_2^2 + s_3^2. \tag{5}$$

3. Results and discussion

In the following, we consider two cases: one with low absorption, the other one with high absorption. The one with low absorption is investigated in more detail, as it is the most probable case to be used for further monochromatizing a SASE beam. With high absorption, the cooling problems are not solvable, which precludes such a reflection being used for monochromators of a SASE beam.

3.1. Low absorption

We take a 220 reflection from a diamond crystal, $\lambda = 1$ Å wavelength, as a typical example. Absorption is very small and can be taken into account by complex values of the Fourier coefficients.

Numerical values of the Fourier coefficients are (Stepanov, 2001)

$$\chi_0 = -9.56 \times 10^{-6} + i\,5.02 \times 10^{-9},$$
$$\chi_h = -3.04 \times 10^{-6} + i\,4.81 \times 10^{-9}.$$

The Bragg angle is $\Theta_B = 23.41°$ and the polarization factor is 0.6843.
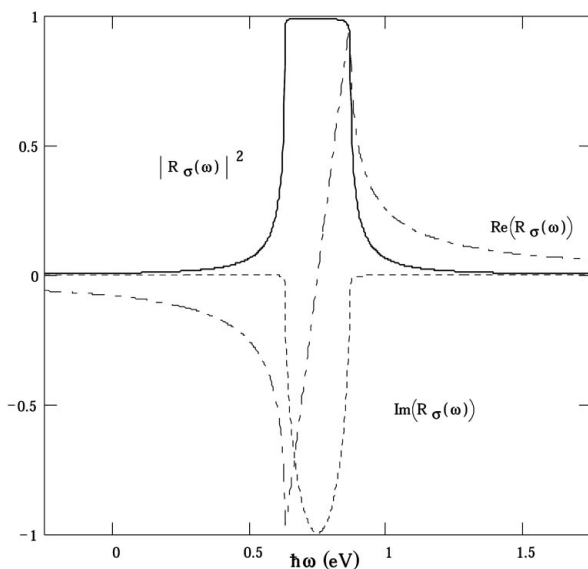

Figure 1
Dependence of the reflectivity R for a symmetric Bragg reflection on energy (diamond 220 at 1 Å wavelength). The complex reflectivity is plotted *versus* the energy, where the energy for an exact Bragg reflection (without refraction) has been subtracted. Also given is the square modulus of the reflectivity, which is the well known Darwin–Prins curve. The subscript σ indicates linear polarization perpendicular to the plane of incidence. This differs from the figure of Shastri *et al.* (2001*a*) (different sign of the real part) because of the different sign of the k vector (Shastri, 2002).

Fig. 1 shows the real and imaginary parts and the square modulus of the reflectivity $R(\omega)$. For the rest of this paper, ω denotes the difference from the central frequency.

As seen from Fig. 1, with low absorption the real part of the reflectivity $R(\omega)$ is antisymmetric about the centre of the reflection curve, whereas the imaginary part is symmetric, if a small asymmetric contribution due to absorption can be neglected. The Fourier transform in the time domain is, therefore, completely imaginary, as seen in the following equations,

$$\int_{-\infty}^{\infty} d\omega \left[R_r(\omega) + iR_i(\omega) \right] \exp(i\omega t) = \int_{0}^{\infty} d\omega \{ R_r(\omega)[\exp(i\omega t) - \exp(-i\omega t)]$$
$$+ iR_i(\omega)[\exp(i\omega t) + \exp(-i\omega t)] \}$$
$$= \int_{0}^{\infty} d\omega\, 2i \left[R_r(\omega) \sin(\omega t) \right.$$
$$\left. + R_i(\omega) \cos(\omega t) \right]. \tag{6}$$

As this holds for both polarization components, the crystal reflection does not change the phase correlation, so the incident relative phase is preserved. This is completely different from a single-plane monochromatic wave where only in the centre of the reflection curve does the relative phase remain unaltered, and, for any angular deviation, an incident wave that is linearly polarized outside the plane of incidence is transformed into an elliptically polarized one.

Fig. 2 shows the amplitude response to a short pulse for both principal directions of linear polarization.

At 0 fs, because of the narrower reflection curve of the π component, a smaller amplitude is seen. At 12 fs, the amplitudes of both components are equal whereas, at about 21 fs, the σ component has dropped to zero and the π component still has an appreciable value. If the σ and π components are coherent, the amplitudes may interfere, in which case the polarization of the reflected beam is no longer constant but varies with time depending on the polarization of the incident radiation.

In the following, we will discuss two exemplary cases, namely linearly polarized light with a polarization direction between the σ and π direction and circularly polarized radiation for a single pulse. We use a single pulse because the effects are shown more clearly but also consider a series of pulses, which better represents the actual emission from a SASE FEL.

3.1.1. Linear polarization. The incident radiation is assumed to be linearly polarized under 45° with respect to the plane of incidence.
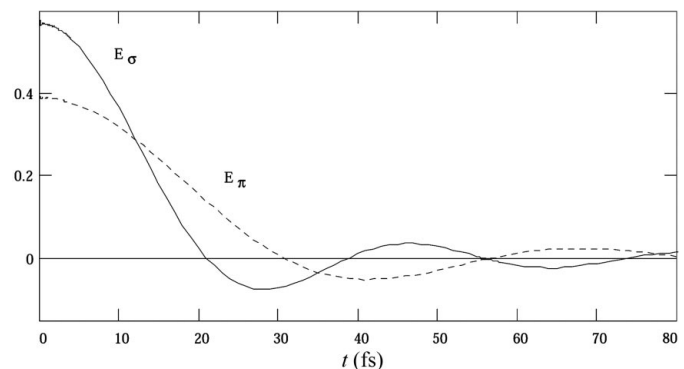

Figure 2
Amplitude response of a diamond 220 reflection to a δ-pulse. Shown are the principal polarization components, namely those perpendicular and parallel to the plane of incidence. The time scale is in femtoseconds and scales simply with the polarization factor, whereas the intensity axis shows arbitrary units. As the π component has a narrower reflection range the integral value is lower.

Polarization exactly perpendicular or parallel to that plane does not show the effects described in the following.

As already mentioned above, for a δ-pulse there is no extra phase shift introduced between the principal polarization components, and the reflected beam remains linearly polarized all the time ($\alpha = 0$). However, owing to the weaker response of the π component, a rotation towards the σ direction occurs immediately at $t = 0$. At larger times, the ratio of the σ to the π component changes and the polarization plane starts to rotate. At 12 fs it has reached 45° again, and at 21 fs pure π polarization dominates. At 32 fs, pure σ polarization occurs. At 40 fs, the reflected beam is again π polarized. By chance, the second zeroing of the π component and the third zeroing of the σ component almost coincide at 55 fs, and the total intensity outside the crystal drops to zero. Inside the crystal though, there is still some energy stored in the vibrating oscillators (atoms). Thus, after 55 fs, some reflected intensity is again observed outside the crystal, but the polarization plane rotates in the opposite direction.

Fig. 3 shows the normalized Stokes parameters s_1 and s_2; s_3 is always zero.

Fig. 4 shows the reflected amplitude and its orientation on the $\sigma\pi$ plane. For a better visualization of the polarization plane, the amplitude is shown in the opposite direction as well.
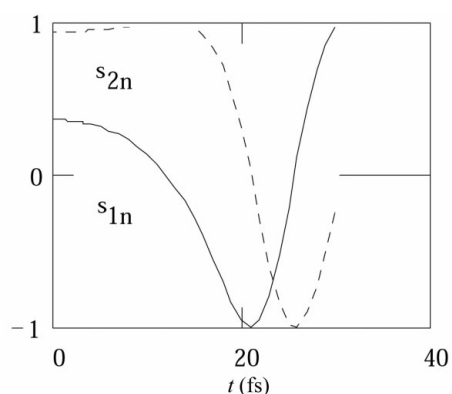
Although the behaviour of a single pulse is interesting in its own right, a real SASE bunch consists of many short pulses with a random phase distribution. Therefore, the effect of a monochromator crystal should be studied under these more realistic conditions. A dataset obtained by Yurkov (2001) contains 15 770 simulated data points with a time spacing of 0.017 fs, thus covering nearly 270 fs, a whole SASE bunch. This dataset was Fourier transformed with a frequency resolution $\Delta\omega = 0.005\ \text{fs}^{-1}$ to obtain the spectral distribution. This spectral distribution was transformed back to the time domain, and the result differed from the original dataset by only a few percent. A histogram of the phases of this dataset shows that the phases are distributed evenly over the interval $[0, 2\pi]$. Fig. 5 contains the intensity distribution of this simulated SASE bunch, and Fig. 6 shows an enlarged section of Fig. 5.

The response of a crystal reflection to such an input is shown in Fig. 7. Again it is assumed that the polarization plane of the input beam is inclined at 45° with respect to the incidence plane of the crystal. The incidence angle of the crystal is chosen in such a way that the much narrower frequency acceptance of the crystal is centred about the frequency distribution of the SASE FEL output. A slight rotation would give a different result but would not influence the (statistical) findings.

Figure 3
Time dependence of the normalized Stokes parameters for linearly polarized light. As mentioned in the text, the normalized Stokes parameters are set to zero where the intensity has dropped below 1% of the maximum intensity, which here is after 30 fs.
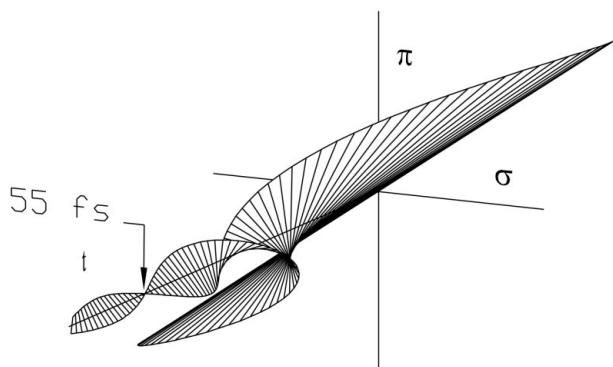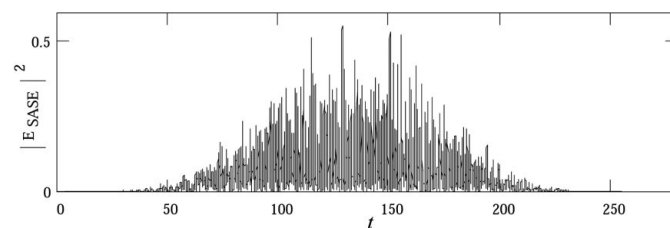

Figure 5
Simulation of the intensity coming out of a SASE FEL (courtesy of M. V. Yurkov). The time axis is in femtoseconds, whereas the intensity axis has arbitrary units.
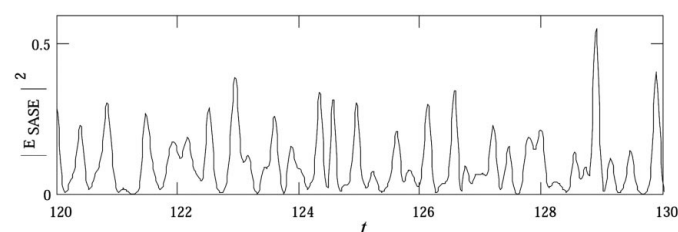

Figure 6
Same as Fig. 5, but with the time axis enlarged.

Figure 4
Linearly polarized incident radiation (single short pulse). Shown is the reflected amplitude in the $\sigma\pi$ plane and its mirror image, to visualize the polarization plane. With time (shown as a third axis perpendicular to the $\sigma\pi$ plane) the polarization plane begins to rotate. At 21 fs the polarization is perpendicular to the plane of incidence, whereas at 32 fs it is parallel to the plane of incidence, and so on.
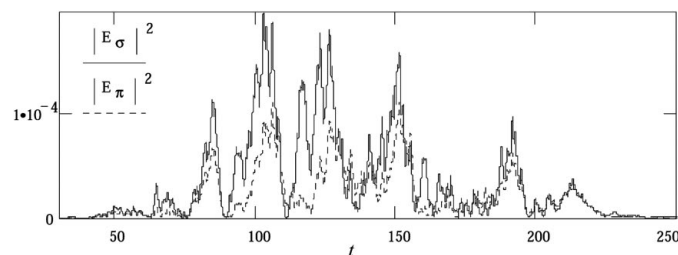

Figure 7
Intensity response to a SASE FEL bunch. Both principal polarization components are shown. Note the relative difference, which cannot be explained by a common scale factor.

Walter Graeff · Time dependence of X-ray pulse polarization

Two remarkable effects are visible. First, the time structure compared with the input has changed drastically. As expected, the short spikes in the input are washed out, but the behaviour is still chaotic. The intensity may eventually drop to zero (*e.g.* at 90 fs or 110 fs in Fig. 7), which would not occur if the intensity distributions are simply convoluted. However, we have to convolute the complex amplitude of the SASE FEL bunch and the time response of the crystal. We can no longer expect the σ and π components to stay in phase, as is the case with the homogeneous frequency distribution of a single pulse, which means that elliptical polarization can occur. This is seen very clearly in Fig. 8, where the time dependence of the Stokes parameters is shown. s_3 is no longer zero but can vary in both directions, indicating right- and left-handed elliptical polarization.

The second point is that the difference between the σ and π components cannot be explained by a common scale factor, for instance, the polarization factor, but the two components may behave in a completely different way, especially on the onset of a burst of reflected radiation.

3.1.2. Circular polarization. The incident wave is assumed to be circularly polarized. Of course, speaking of a δ-pulse as being circularly polarized does not make sense. However, as a pulse width of 0.1 fs 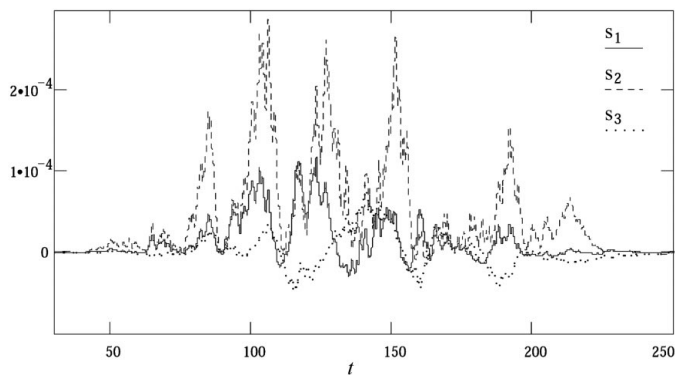(still hundreds of wavelengths long) behaves almost like a δ-pulse (see discussion above), we assume that with a sufficiently long pulse the property of circular polarization is meaningful. The Stokes parameters show the same time behaviour if s_2 and s_3 are interchanged, therefore Fig. 3 would be unaltered if we replaced s_3 with s_2. This is because $\alpha = 0$ describes linear polarization and $\alpha = 90°$ describes circular polarization.

Because the amplitude of the σ component has dropped to zero at 21 fs, the outgoing radiation at that moment is linearly polarized in the π direction. Afterwards, the outgoing radiation is elliptically polarized again until, at 32 fs, the opposite happens and the wave is linearly polarized in the σ direction, and so on (see Fig. 9).

A simulated SASE FEL bunch coming out of a helical undulator was not investigated, but a similarly chaotic behaviour to that described above can be expected.

3.2. High absorption

We take the 220 reflection from a silicon crystal, $\lambda = 2$ Å wavelength, as a typical example. Absorption is quite high and, again, can be taken into account by complex values of the Fourier coefficients.

Numerical values of the Fourier coefficients are (Stepanov, 2001)

$$\chi_0 = -2.56 \times 10^{-5} + i\,0.97 \times 10^{-6},$$
$$\chi_h = -1.56 \times 10^{-5} + i\,0.92 \times 10^{-6}.$$

The Bragg angle is $\Theta_B = 31.39°$ and the polarization factor is 0.4575.

Fig. 10 shows the reflectivity curve. A comparison with Fig. 1 shows the influence of absorption clearly. Nevertheless, at a first glance the overall symmetry has not changed.

At a second glance, the real part in particular shows an asymmetry. Therefore, (6) is no longer valid and, consequently, for a linearly polarized incident wave, the Stokes parameter s_3 is no longer zero at all times, as seen in Fig. 11.

The behaviour of s_{1n} and s_{2n} is very similar, at least up to the first minimum, as in the case of no absorption. However, roughly 10 fs after the onset of the pulse the Stokes parameter s_{3n} has non-zero values, which indicates elliptical polarization. Taking the formulae given by Born & Wolf (1997), we may estimate the eccentricity of this elliptical polarization. Born & Wolf introduce an auxiliary angle χ

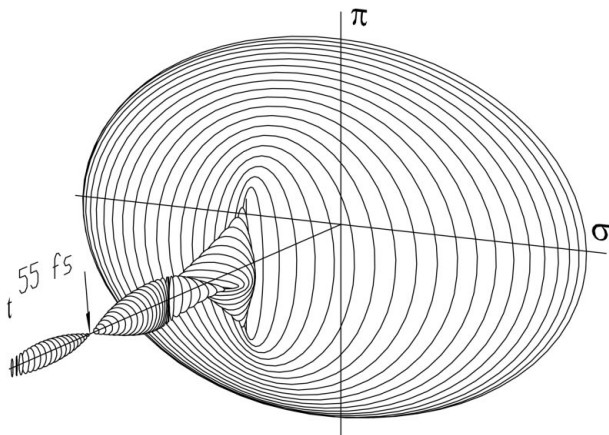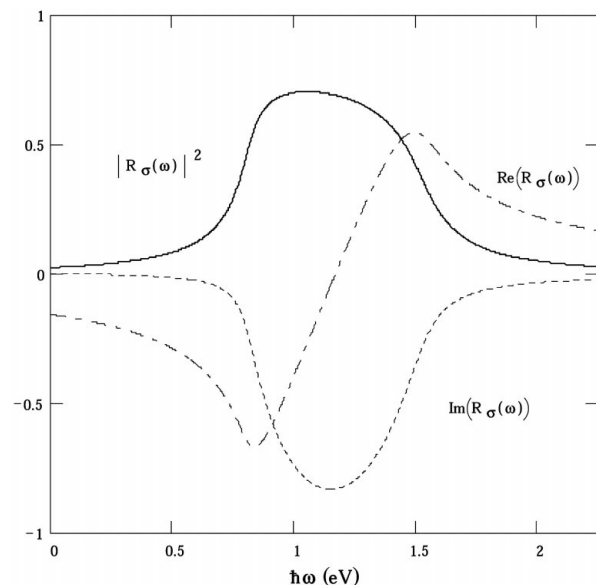**Figure 8**
Time dependence of the Stokes parameters.

Figure 9
Circularly polarized incident radiation. Shown is the reflected amplitude on the $\sigma\pi$ plane. With time, the amplitude rotates in this plane quite rapidly. For clarity, the resulting spiral is not shown completely, but its cross section is shown every femtosecond. After 21 fs the reflected radiation is linearly polarized perpendicularly to the plane of incidence. At 32 fs the polarization is again linear but rotated about 90°, and so on. Note again the drop of the intensity to zero at 55 fs and its subsequent reappearance.

Figure 10
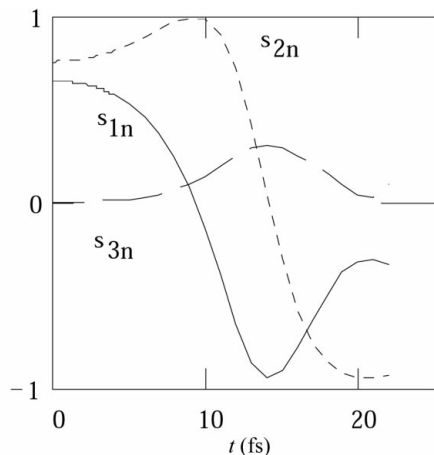Reflectivity curve of a silicon 220 reflection at 2 Å wavelength. Compare with Fig. 1.

Figure 11
Time dependence of the normalized Stokes parameters for linearly polarized light. Compare with Fig. 3. Note that, with absorption, s_3 after some time is no longer zero.

The aim of this paper is to sensitise experimentalists to the rather strange effects on the polarization of short X-ray pulses when they are reflected.

As the reflected amplitudes of an incident δ-pulse cross zero several times, the polarization of the reflected beam is time dependent as well, as soon as a mixture of both components is present, especially with elliptical polarization. This effect should certainly be taken into account when polarization-sensitive experiments are planned. Fortunately, this effect is small for a single pulse, as the intensity in the interesting region has dropped to just a few percent. In addition, in the case of linear polarization, the mixture of both principal components can easily be avoided. This is true for the two-beam and coplanar many-beam cases only. In the case of elliptical polarization, however, in combination with a chaotic series of pulses, the polarization effects may assume unexpected values.

(which should not be confused with the dielectric susceptibility) and give

$$
\begin{aligned}
s_{3n} &= \sin(2\chi), \\
\tan(\chi) &= a/b,
\end{aligned}
\tag{7}
$$

where a/b is the aspect ratio of the ellipse. In our case, after about 15 fs, s_{3n} reaches its maximum value of 0.4, which corresponds to an aspect ratio of 0.2. In addition to the rather low aspect ratio, the intensity of the pulse has dropped to only a few percent.

4. Conclusion

Owing to the different interaction strengths of the σ and π components expressed by the polarization factor C, the time response of both components is different.

References

Born, M. & Wolf, E. (1997). *Principles of Optics*, 6th ed. Cambridge University Press.
DESY (1997). Report DESY 1997–048, ECFA 1997–182. Deutsches Elektronen-Synchrotron DESY, Hamburg, Germany.
Shastri, S. D. (2002). Private communication.
Shastri, S. D., Zambianchi, P. & Mills, D. M. (2001*a*). *Proc. SPIE*, **4143**, 69–77.
Shastri, S. D., Zambianchi, P. & Mills, D. M. (2001*b*). *J. Synchrotron Rad.* **8**, 1131–1135.
SLAC (1998). Report SLAC-R-521, UC-414. Stanford Linear Accelerator Center, CA 94025, USA.
Stepanov, S. (2001). Values obtained from http://sergey.bio.aps.anl.gov.
Yurkov, M. V. (2001). Private communication.